Available online at www.sciencedirect.com
SCIENCE DIRECT
Journal of Photochemistry and Photobiology A: Chemistry 175 (2005) 129–137
Journal of Photochemistry and Photobiology A:Chemistry
www.elsevier.com/locate/jphotochem

Nifedipine and nitrendipine reactivity toward singlet oxygen

Nancy A. Pizarro-Urzúa*, Luis J. Núñez-Vergara

Laboratorio de Bioelectroquímica, Departamento de Química Farmacológica y Toxicológica, Facultad de Ciencias Químicas y Farmacéuticas, Universidad de Chile, P.O. Box 233, Santiago, Chile

Received 1 February 2005; received in revised form 8 April 2005; accepted 19 April 2005
Available online 31 May 2005

Abstract

The ability to generate singlet molecular oxygen, $O_2(^1\Delta_g)$, and the scavenging activity of two well-known 1,4-dihydropyridines (1,4-DHPs) such as nifedipine (1,4-dihydro-2,6-dimethyl-4-(2-nitrophenyl)-3,5-pyridine-dicarboxylic acid dimethyl ester) and nitrendipine (1,4-dihydro-2,6-dimethyl-4-(3-nitrophenyl)-3,5-pyridine-dicarboxylic acid ethyl methyl ester) is assessed.

Results show that nifedipine does not generate $O_2(^1\Delta_g)$ under our experimental conditions. In contrast, this 1,4-dihydropyridine behaves as a good scavenger of excited oxygen, mainly via physical deactivation with values of the total rate constant ranging from $20.8 \times 10^5\ M^{-1}\ s^{-1}$ in dioxane to $93.0 \times 10^5\ M^{-1}\ s^{-1}$ in propylencarbonate. The less favored reactive pathway generates a photooxidation product, which has been isolated and identified by GC–MS as the nitropyridine derivative. Voltammetric experiments also confirm the generation of this oxidation product.

On the other hand, nitrendipine yields $O_2(^1\Delta_g)$, but it is a less efficient scavenger of this species. Rate constants range from $1.88 \times 10^5\ M^{-1}\ s^{-1}$ in ethyl acetate to $15.8 \times 10^5\ M^{-1}\ s^{-1}$ in *N*,*N*-dimethylacetamide, the reactive channel being the main $O_2(\Delta_g)$ deactivation pathway.

Dependence on solvent microscopic parameters of the total rate constant for the reaction between singlet oxygen and 1,4-DHPs permits us to propose a mechanism involving a perepoxide-like encounter complex in the first step of the reaction path.

Keywords: Nifedipine; Nitrendipine; Singlet oxygen; Phototoxicity; Photosensitized activity

1. Introduction

1,4-Dihydropyridines (1,4-DHPs), calcium channel antagonists, display a well-known cardiovascular activity due to the inhibition of L-type Ca^{+2} channels, which results in a reduced calcium influx with impaired electromechanical coupling both in vascular smooth muscle cells and in the heart. Specifically, 1,4-DHPs are important drugs in the treatment of hypertension and coronary heart disease [1,2]. In addition to these therapeutic applications, other biological activities such as modulation of endothelial function [3], release of nitric oxide [4] and scavenging of some oxygen-derived free radicals [5–8] have been recognized.

Oxygen is an abundant element with multiple faces. Its most common and important one is the molecular form (O_2), which is a prerequisite for all aerobic cell metabolism. Another face of oxygen is the one with an unpaired electron, the free radical derivative with its highly unstable and reactive forms. These reactive forms have been involved in a wide range of toxic mechanisms in biological organisms. When the ground state of oxygen is excited to a higher energy state, singlet molecular oxygen, $O_2(^1\Delta_g)$, is formed. This form of oxygen is a harmful species in biological systems [9]. Thus, singlet oxygen reacts with a great variety of biological molecules such as DNA, proteins and lipids [10–12]. Also, it is genotoxic [13], mutagenic and causes single-strand breaks in DNA, reacting preferentially with the guanine moiety to yield 8-oxo-7,8-dihydroxy-deoxyguanosine [14,15]. Furthermore, singlet oxygen can inactivate viruses and may be involved in the host defense against viruses and bacteria. Another role of singlet oxygen, the activation of gene expression, has also been observed even at concentrations below those required for cytotoxicity [16–18].

* Corresponding author. Tel.: +56 2 6782865; fax: +56 2 6782868.
E-mail address: npizarro@ciq.uchile.cl (N.A. Pizarro-Urzúa).

1010-6030/$ – see front matter © 2005 Elsevier B.V. All rights reserved.
doi:10.1016/j.jphotochem.2005.04.027

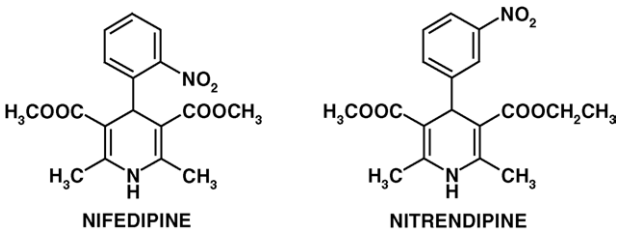

Fig. 1. Chemical structures of nifedipine and nitrendipine.

Some previous reports suggest that nifedipine may be phototoxic in human skin [19,20], but in such studies no mechanisms have been described for this possible toxic effect. Later, Gibbs et al. [21] demonstrated that nifedipine produces phototoxicity in vitro partially mediated by initial formation of a toxic photoproduct, but paradoxically, subsequent UVA irradiation reduces phototoxicity. On the other hand, nifedipine concentrations required to induce in vitro toxicity are much greater than therapeutic plasma levels. To our knowledge, in the case of nitrendipine no studies about its phototoxicity have been yet reported. In view of the fact that singlet oxygen can be formed by energy transfer from an excited photosensitizer and considering the above discussed toxic effects of nifedipine, in this paper we explore both the feasibility of formation of singlet oxygen and its reactivity with both nifedipine and nitrendipine (Fig. 1).

2. Experimental

2.1. Drugs and reagents

Nifedipine (1,4-dihydro-2,6-dimethyl-4-(2-nitrophenyl)-3,5-pyridine-dicarboxylic acid dimethyl ester) and nitrendipine (1,4-dihydro-2,6-dimethyl-4-(3-nitrophenyl)-3,5-pyridine-dicarboxylic acid ethyl methyl ester) were purchased from Sigma.

5,10,15,20-Tetraphenyl-21H,23H-porphine (TPP), 9,10-dimethylanthracene (DMA), phenalenone and 1,3-diphenylisobenzofurane (DPBF) (Aldrich) were used without further purification.

Rose Bengal (RB) (Fluka) was recrystallized from ethanol prior to use. All solvents (Merck) were of spectroscopic or HPLC grade.

2.2. Apparatus and procedures

UV–vis absorption spectra and steady state competitive kinetic experiments were performed in a Unicam UV-4 spectrophotometer. A GC–MS system with a Hewlett-Packard Ultra-2 capillary column (25 m) was used to obtain electron impact mass spectra.

Chemical reaction rate constants were determined in several selected solvents using a 10 mL double-wall cell, light-protected by black paint. A centered window allowed irradiation with light of a given wavelength by using appropriate cut-off filters. Circulating water maintained the cell temperature at $22 \pm 0.5\,^{\circ}C$. Sensitizer irradiation (RB or TPP) was performed with a visible, 200 W, Par lamp. A gas chromatograph equipped with a NPD detector and a Hewlett-Packard Ultra-2 capillary column was used to monitor substrate consumption. DMA and DPBF were used as actinometers.

Time-resolved luminescence measurements were carried out in 1 cm pathlength fluorescence cells. TPP or RB was excited by the second harmonic (532 nm, nominal power ca. 9 mJ per pulse) of a 6-ns light pulse of a Quantel Brilliant Q-Switched Nd:YAG laser. A liquid-nitrogen cooled North Coast germanium photodiode detector with a built-in preamplifier was used to detect infrared radiation from the cell. The detector was at a right-angle to the cell. An interference filter (1270 nm, Spectrogon US, Inc.) and a cut-off filter (995 nm, Andover Corp.) were the only elements between the cell face and the diode cover plate. Preamplifier output was fed into the 1 MΩ input of a digitizing oscilloscope. Computerized experiment control, data acquisition and analysis were performed with LabView-based software developed at the Laboratory of Kinetics and Photochemistry of the University of Chile.

Laser flash photolysis was performed with a Q-switched Nd:YAG laser (532 nm, ca. 9 mJ per pulse). A 150-W Xe lamp mounted in a lamp housing system was employed as the monitoring light beam. The lamp beam was passed through a water filter before impinging on the entrance of the cell holder. An electronic shutter, controlled by a shutter driver/timer, was placed between the water filter and the cell holder. The shutter was triggered by the Q-switch from the laser. Two lenses and slits were used to collimate and focus the monitoring light to the cell holder and to the entrance slit of the monochromator. A photomultiplier detector mounted in a homemade housing was fitted to the monochromator exit slit port. PMT signals were monitored with a 500-MHz digital oscilloscope. An external PTI optical beam divider was employed to trigger the oscilloscope. The signals can be stored and averaged in the same scope at the repetition rate of the laser pulse (10 Hz) or can be fed to a personal computer equipped with home-designed software for data acquisition and treatment.

Singlet oxygen quantum yields (ϕ_{Δ}) were measured in time-resolved phosphorescence experiments using phenalenone as the actinometer ($\phi_{\Delta} = 0.98$ in acetonitrile, $\phi_{\Delta} = 0.93$ in benzene and $\phi_{\Delta} = 0.97$ in ethanol) [22], by comparing the response of the detector extrapolated at zero time and zero laser power, the latter adjusted with a set of neutral density filters. Samples and actinometer were both excited by the third harmonic (355 nm, ca. 28 mJ per pulse) of the Nd:YAG laser.

Equation coefficients and statistical parameters of LSER correlations were obtained by multilinear correlation analysis with STAT VIEW 5.0 (SAS Institute Inc.). Results agreed with the *t*-statistic of descriptors.

Cyclic Voltammetry (CV) and Differential Pulse Voltammetry (DPV) experiments were performed in a Metrohm® 693 VA Processor equipped with a voltammetric stand 694 VA. A Pentium III Gateway microcomputer was used for

data control, acquisition and treatment. The operating conditions for DPV experiments were as follows: pulse amplitude, 40 mV; potential scan, 4 mV s^{-1}; voltage range, −50 to 1200 mV and 0–1000 mV; current range, 5–25 mA, temperature, 25 °C. All the solutions were purged with pure nitrogen for 10 min before the voltammetric runs. A Metrohm hanging mercury electrode (HMDE) with a drop surface of 1.90 mm^2 for CV, and a glassy carbon electrode for DPV as working electrode and a platinum wire as a counter electrode were used. All potentials were measured against a saturated calomel reference electrode (SCE).

3. Results and discussion

3.1. Generation of singlet oxygen by 1,4-DHP derivatives

The ability of these two 1,4-DHPs to form singlet oxygen, $O_2(^1\Delta_g)$, was assessed by using the phosphorescence method [23]. Fig. 2 shows the decay of the luminescence of $O_2(^1\Delta_g)$ at 1270 nm, after the excitation of either nitrendipine or nifedipine with pulses of third harmonic of the Nd-YAG laser at 355 nm. As can be seen from this figure, no $O_2(^1\Delta_g)$ emission was observed for nifedipine, thus this compound does not generate excited oxygen as nitrendipine does. In Table 1, the quantum yields (ϕ_Δ) for $O_2(^1\Delta_g)$ generation by nitrendipine are displayed. The evaluated quantum yield was dependent on laser power as shown in Fig. 3, indicating the existence of nonlinear phenomena. In addition, the quantum yields are concentration-independent; therefore, deactivation of the excited states by molecules in the ground state can be discarded. However, generation of $O_2(^1\Delta_g)$ is solvent-dependent, being more efficient in an apolar solvent such as benzene. This result is important considering that 1,4-DHP derivatives can accumulate in membranes due to their lipophilic nature [24], which leads to more efficient singlet oxygen generation by nitrendipine in a biological system.

Table 1
Quantum yields of $O_2(^1\Delta_g)$ generation by nitrendipine photosensitization

Solvent	Absorbance	ϕ_Δ
Acetonitrile	0.625	0.025 ± 0.002
	0.638	0.020 ± 0.001
Benzene	0.610	0.046 ± 0.003
	0.308	0.038 ± 0.003
Ethanol	0.654	$<10^{-3}$

Although a triplet biradical involved in the photolysis of nifedipine has been reported [25], excited triplet states of the 1,4-DHPs under study were not observed in the employed experimental conditions. This species would be generated from a photoinduced intramolecular electron transfer followed by fast hydrogen abstraction by the excited nitro group with concomitant consumption of the 1,4-DHP derivatives [25]. Consequently, the *ortho* position of the nitro moiety in the 4-aryl substituent is responsible for the fast photodegradation of nifedipine, preventing the possibility of singlet oxygen generation. Conversely, the *meta* position of the nitro group in nitrendipine (far from abstractable hydrogen) permits the existence of a longer lived transient capable of producing excited oxygen. These results could indicate that the photoallergic and phototoxic effects produced by these two drugs have different mechanisms, considering that nitrendipine generates singlet oxygen but nifedipine does not.

3.2. Interaction of 1,4-DHP derivatives with singlet oxygen

The total (physical and chemical) quenching rate constants, k_T, for the reaction of $O_2(^1\Delta_g)$ with nifedipine and nitrendipine in several solvents were determined using time-

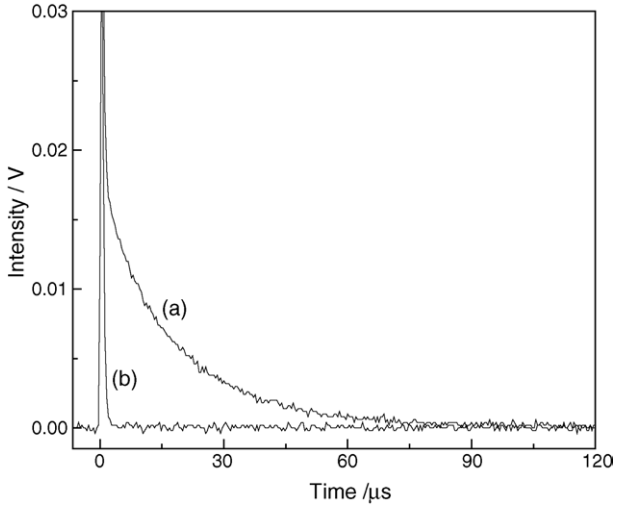

Fig. 2. Luminescence decay of $O_2(^1\Delta_g)$ at 1270 nm, generated after the excitation at 355 nm of (a) nitrendipine and (b) nifedipine with third harmonic pulses of Nd-YAG laser.

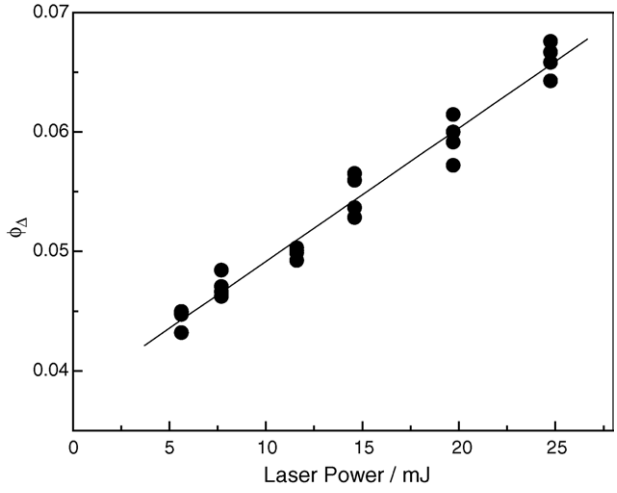

Fig. 3. Quantum yield of the photosensitized generation of $O_2(^1\Delta_g)$ by nitrendipine in benzene, as a function of the power of the excitation source.

resolved phosphorescence detection (TRPD). $O_2(^1\Delta_g)$ lifetimes were evaluated in the absence (τ_0^{-1}) and in the presence (τ^{-1}) of each 1,4-dihydropyridine, and k_T was obtained according to a Stern–Volmer treatment ($\tau^{-1} = \tau_0^{-1} + k_T$[1,4-DHP]). Linear plots of τ^{-1} versus [1,4-DHP] were obtained in all solvents employed and intercept of these plots match closely with reported singlet oxygen lifetime [26].

Quenching of excited states of sensitizers by 1,4-DHPs may be disregarded, since singlet or triplet deactivation was not observed under our experimental conditions. To prevent participation of nifedipine photoproducts in quenching experiments, new solutions were prepared for each measurement, avoiding unnecessary irradiation of the solutions.

The k_T values in different solvents are tabulated in Table 2 and the errors are within 10% for all results. A clear divergence of reactivities for both compounds can be observed. Total quenching rate constants for nifedipine were one order of magnitude higher than those for nitrendipine, increasing 4.5-fold from dioxane to propylenecarbonate, while the constant corresponding to nitrendipine increased 10-fold from chloroform to dimethylacetamide. Fig. 4 shows the solvent effect on k_T for both 1,4-DHPs.

The chemical quenching rate constants, k_R, for the 1,4-DHPs were determined in several selected solvents employing TPP as the sensitizer and the drug consumption was monitored by gas chromatography. DMA and DPBF were used as actinometers to determine the steady-state $O_2(^1\Delta_g)$ concentration. Values of k_R were obtained from slopes of pseudo-first-order plots, which are summarized in Table 2. As can be seen from this table, k_R for both 1,4-DHPs are similar in the tested solvents, being higher for nitrendipine in acetonitrile, ethanol and propylenecarbonate. Also, the kinetic rate constants (k_T or k_R) for both 1,4-DHPs show the same dependence on the solvent polarity. Thus, k_T values increase in solvents with ability to stabilize charges or dipoles, suggesting that an intermediate or transition state with polar character is involved.

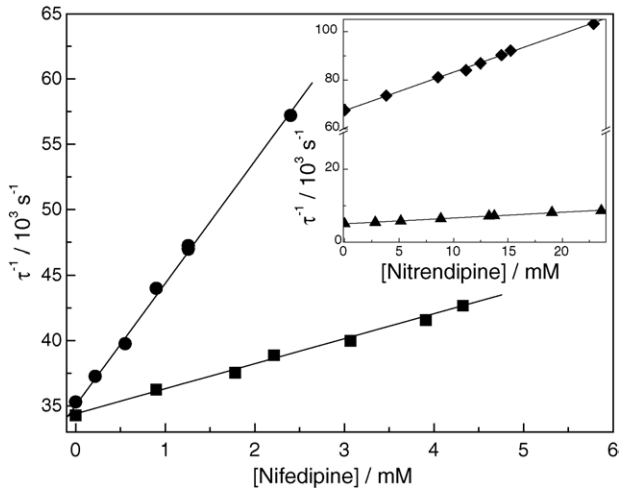

Fig. 4. Stern–Volmer plot for deactivation of singlet oxygen by nifedipine (■) in benzene (●) in propylencarbonate. Inset: Stern–Volmer plot for deactivation of singlet oxygen by nitrendipine (▲) in chloroform (♦) in dimethylacetamide.

The k_R/k_T ratio values have been related with the balance between the biological damage and the protector effect of singlet oxygen [28]. Comparison of the k_R/k_T ratio in different solvents (Table 3), shows higher values for nitrendipine in all cases. Nifedipine has k_R/k_T ratio values lower than 9%, meaning that most of the singlet oxygen is scavenged by physical quenching. This behaviour is similar to the one reported for other biomolecules considered as effective antioxidants, i.e. they quench singlet oxygen mainly by physical deactivation [27]. However, nitrendipine k_R values are close to k_T values, indicating that the main deactivation path of $O_2(^1\Delta_g)$ is the channel leading to reaction products. Then, nifedipine protector effect in biological systems would be greater than that of nitrendipine.

The dye-sensitized photooxygenations of both 1,4-DHPs under study yield the corresponding 4-nitroaryl pyridine derivative as the main product. These isolated products were

Table 2
Total quenching (k_T) and chemical quenching (k_R) rate constants for reactions of 1,4-DHP derivatives with singlet oxygen in different solvent

Solvent	Nifedipine		Nitrendipine	
	k_T ($\times 10^5$ M^{-1} s^{-1})	k_R ($\times 10^5$ M^{-1} s^{-1})	k_T ($\times 10^5$ M^{-1} s^{-1})	k_R ($\times 10^5$ M^{-1} s^{-1})
Ethyl acetate	–	–	1.88	–
Dioxane	20.8	–	2.26	–
Benzene	22.0	0.08	2.67	0.09
Chloroform	36.6	–	1.55	0.18
Methylene chloride	43.7	–	8.26	–
Acetonitrile	50.0	0.41	4.94	1.14
Methanol	82.5	–	5.44	–
Ethanol	68.9	0.38	2.10	0.97
Acetone	69.7	–	2.91	–
n-Propanol	74.3	–	3.66	–
N,*N*-Dimethylformamide	82.5	6.97	8.15	6.20
N,*N*-Dimethylacetamide	60.7	–	15.8	–
Propylencarbonate	93.0	3.98	11.6	5.66

Table 3
Ratio between chemical and total rate constant for reactions of nifedipine and nitrendipine with singlet oxygen

Solvent	Nifedipine k_R/k_T	Nitrendipine k_R/k_T
Benzene	0.004	0.03
Chloroform	–	0.12
Acetonitrile	0.008	0.23
Ethanol	0.005	0.46
N,*N*-Dimethylformamide	0.084	0.76
Propylencarbonate	0.043	0.49

characterized and identified by GC–MS analysis, Differential Pulse Voltammetry and Cyclic Voltammetry.

Fig. 5 shows a typical GC–MS chromatogram corresponding to a 1, 4 mM solution of nifedipine in acetonitrile irradiated for 53 h in the presence of TPP. The main peak in the chromatogram has a retention time of 8.61 min, which corresponds to the unreacted 1,4-DHP (Fig. 5a). In Fig. 5b, the corresponding mass spectrum is shown. The peak with a retention time of 6.02 min belongs to the main product of photosensitized oxidation of nifedipine, i.e. the pyridine derivative, whose mass spectrum is shown in Fig. 5c.

Complementary electrochemical experiments were also performed in order to confirm the functionality present in the structure of the reaction products resulting from 1,4-DHPs and singlet oxygen. In Fig. 6a, a typical differential pulse voltammogram of 1.45 mM nifedipine solution in aqueous buffer solution at pH 7 is shown. The anodic peak at 793 mV versus SCE corresponds to the oxidation of the 1,4-dihydropyridine ring to yield the pyridine derivative. Fig. 6b

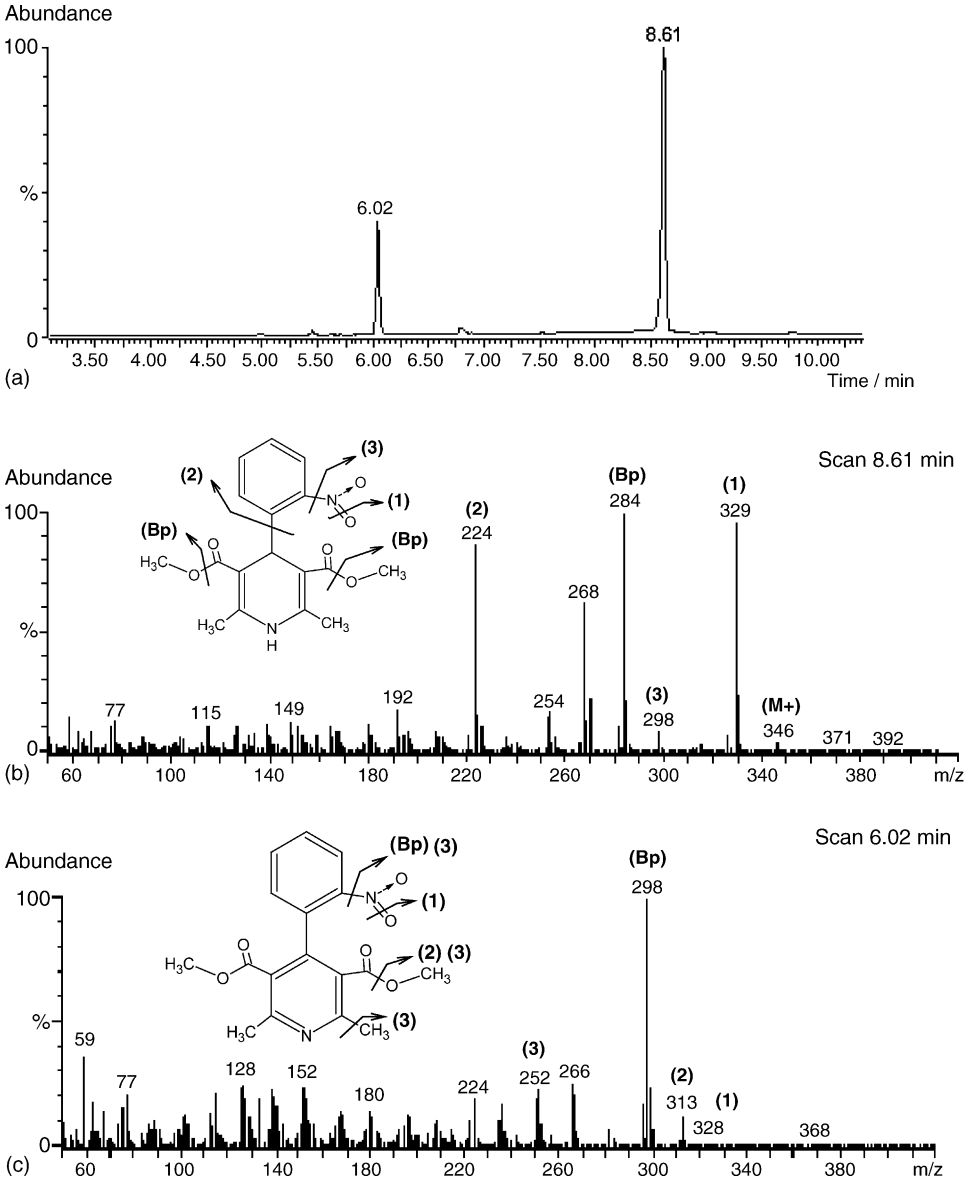

Fig. 5. (a) GC–MS chromatogram of 1.4 mM nifedipine in acetonitrile after 53 h of irradiation in the presence of TPP; (b) EI + mass spectrum of nifedipine; (c) EI + mass spectrum of nitro-pyridine derivative.

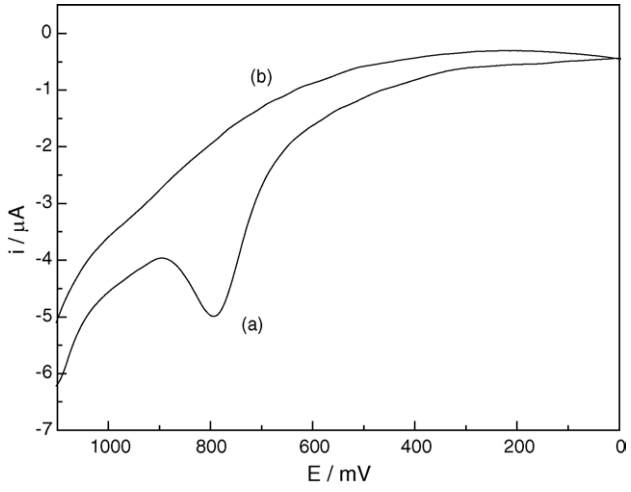

Fig. 6. Differential pulse voltammograms of: (a) 1.45 mM nifedipine solution, and (b) 1 mM solution of the isolated product from the reaction between nifedipine and singlet oxygen. Working electrode: glassy carbon electrode.

shows a differential pulse voltammogram of a 1 mM solution of the isolated product of the reaction between nifedipine and singlet oxygen. This experiment indicated that the 1,4-dihydropyridine moiety is not present in the reaction product structure as shown by the absence of the original anodic signal at 793 mV versus SCE.

A typical cyclic voltammogram on Hg for 1.45 mM nifedipine solution is shown in Fig. 7a. The reduction of the nitro group produces a cathodic peak at −633 mV versus SCE. Fig. 7b shows a cyclic voltammogram corresponding to a 1 mM solution of the isolated product of the reaction between nifedipine and singlet oxygen. It is clear that this last derivative maintains the nitro group in its structure, since the original reduction signal at −633 mV is present. The dissimilar heights observed for both peaks are due to the different initial concentration of the compounds.

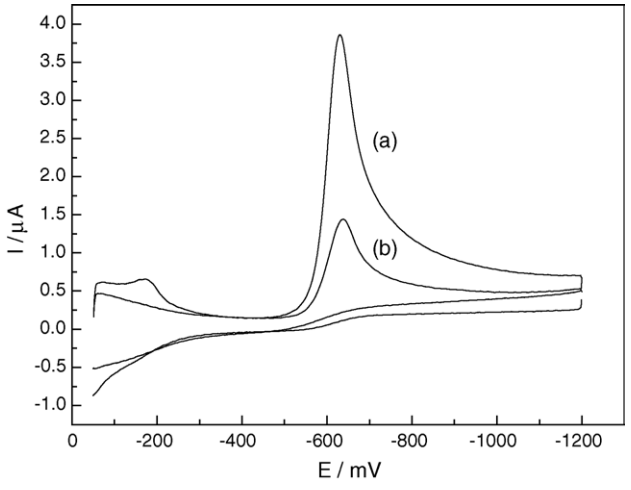

Fig. 7. Cyclic voltammograms of: (a) 1.45 mM nifedipine solution and (b) 1 mM solution of the isolated product from the reaction between nifedipine and singlet oxygen. Working electrode: hanging mercury dropping electrode (HMDE).

Nifedipine is the more reactive compound toward singlet oxygen. This drug exhibits a more positive oxidation peak potential than nitrendipine, i.e. it is more difficult to be oxidized. Therefore, an electron transfer reaction in the first step of the reaction path could be discarded. Nevertheless, glassy carbon electrode voltammetric experiments show a direct relation between the potential peak values and the electronic density on the dihydropyridine ring [29].

In order to obtain more information about the type of interaction involved in the first step of the reaction between 1,4-DHPs and $O_2(^1\Delta_g)$, we analyzed the rate constant dependence on the empiric microscopic parameters of the solvent [30], by using the semi empirical solvatochromic equation (LSER) of Kamlet et al. [31,32]:

$$\text{Log}\, k = \log\, k_0 + a\alpha + b\beta + s\pi^* + \text{d}\delta + h\rho_{\text{H}}^2 \quad (1)$$

where α is the hydrogen bond donation (HBD) ability of the solvent, β is the hydrogen bond acceptance (HBA) or electron pair donation ability to form a coordinative bond, and π^* is the polarity/polarizability parameter. The parameter δ is a correction term for polarizability, which takes values equal to 1.0 for aromatic solvents, 0.5 for polyhalogenated aliphatic solvents, and 0 for all other aliphatic solvents. The Hildebrand's solubility parameter, ρ_{H}, corresponds to the square root of the solvent cohesive density and is a measure of the disruption of solvent–solvent interactions in creating a solute cavity. The solvent-independent coefficients a, b, s, d and h are characteristic of the process and indicative of the rate constant sensitivity to each solvent property, accounting for the established specific interactions at microscopic level between solute and solvent during the formation/stabilization of the encounter complex (exciplex in some cases).

The coefficients of the LSER equation obtained by multilinear correlation analysis for the dependence of k_{T} on sol-

Table 4
LSER correlation equations for the reaction of singlet oxygen with nifedipine and nitrendipine

	$\log k = \log\, k_0 + s\pi^* + \text{d}\delta + h\rho_{\text{H}}^2$			
	$\log k_0$	s	d	h
Nifedipine				
Coefficient	6.278	0.317	−0.277	0.002
±	0.208	0.213	0.113	0.001
t-stat	30.224	1.486	−2.446	2.473
P (two-tail)	<0.0001	0.1755	0.0402	0.0385
VIF		1.316		1.316
$N = 12$, $R = 0.901$, S.D. = 0.097, $F = 11.523$				
Nitrendipine				
Coefficient	4.012	1.917	–	0.002
±	0.229	0.297		0.002
t-stat	17.557	6.463		2.436
P (two-tail)	<0.0001	<0.0001		0.0351
VIF		1.316		1.316
$N = 13$, $R = 0.916$, S.D. = 0.142, $F = 26.134$				

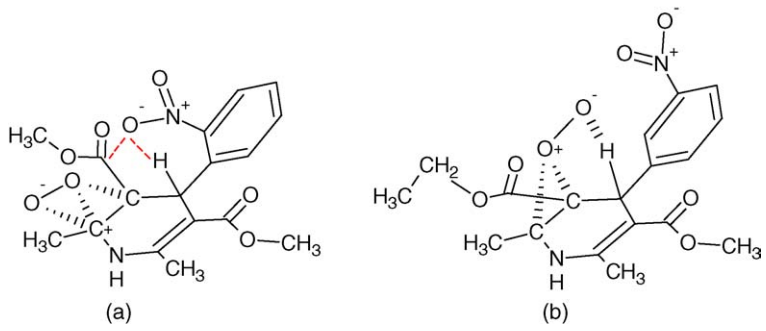

Fig. 8. Proposed encounter complex formed in the first step of the reaction of singlet oxygen with (a) nifedipine and (b) nitrendipine.

vent parameters are given in Table 4. These values result from purely statistical criteria. The overall quality of equation is indicated by sample size, N, correlation coefficient, R, standard deviation, S.D., and Fisher index of equation reliability, F. The reliability of each term is indicated by a large t-statistics, t-stat, two-tail probability, P(two-tail) < 0.05; and the VIF statigraph (a measure of parameter orthogonally) is near to one. Good quality is indicated by large N and F values, small S.D. and R close to one. Results show that not all the descriptors are significant. Descriptor coefficients accepted in the correlation equation were those with a significance level $\geq$0.95. For this reason, α and β parameters were not included in the LSER correlation. According to the coefficients of the equations in Table 4, the k_T values for both 1,4-DHPs increase in solvents with the largest capacities to stabilize charges and dipoles, and increase in solvents with high cohesive energy.

The rate constant dependence on the π^* parameter could account for the participation of an encounter complex with charge separation. The influence of Hildebrand's solubility parameter, ρ_H, could indicate that liberation of solvent molecules occurs in the formation of this complex. This dependence (the same for both compounds) can be interpreted in terms of the formation of a perepoxide-like encounter complex due to the attack of singlet oxygen on the carbon=carbon double bond. The participation of this kind of exciplex has been widely supported by many previous experimental results [33,34] and also by theoretical calculations [35]. For nitrendipine, the perepoxide-like exciplex could be stabilized by an intramolecular interaction of allylic hydrogen (like the one in the 4-position of dihydropyridine ring) with the negatively charged terminal oxygen. For nifedipine, this type of stabilization would be hindered by the presence of *ortho*-nitroaryl substituent, since it has been established that the *ortho*-nitro function is at reaction distance from the labile hydrogen (H–C_4) and the ester moiety [25]. This interaction could be responsible for a higher charge density on the dihydropyridine ring with the concomitant greater nifedipine reactivity toward singlet oxygen. The lower effect of the solvent on the nifedipine rate constant could be attributed to the interaction between the nitro group and the hydrogen in the 4-position, the perepoxide would be stabilized through the interaction of negatively charged oxygen with the carbon atom adjacent to the amino group, adopting a geometry denominated perepoxide-like zwitterion. This kind of encounter complex has been proposed for the reaction of singlet oxygen with enol ethers and enamines [35]. Both proposed exciplexes

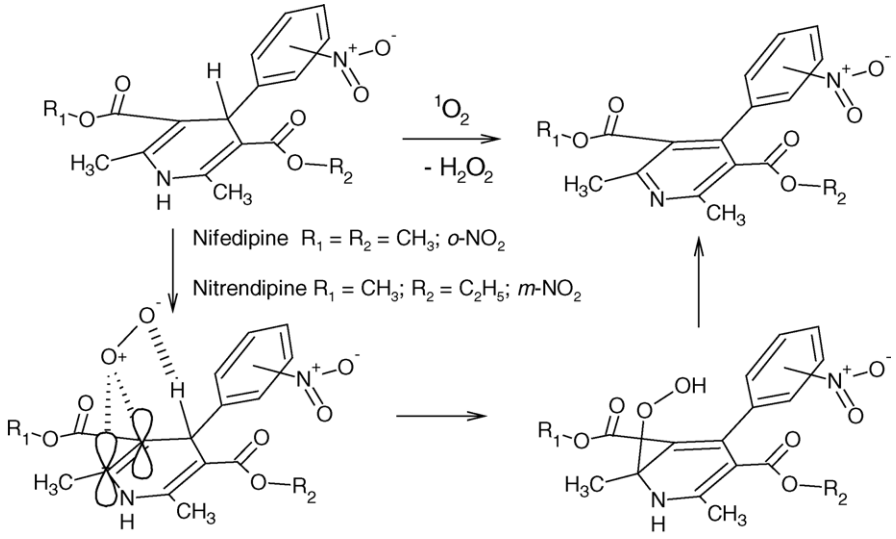

Fig. 9. Proposed mechanism for the reaction of $O_2(^1\Delta_g)$ with nitrendipine and nifedipine.

are shown in Fig. 8. Although in both encounter complexes (nifedipine, nitrendipine) partial separation of charges is produced, in the case of the latter, this process is more relevant, considering that the coefficient associated to the π^* parameter is significantly higher than in the case of nifedipine. This result can be explained by the preferential geometry adopted due to the greater availability of the labile hydrogen (H–C_4) in the dihydropyridine ring, producing more formal charge separation. The dependence on the ρ_H parameter accounts for a more compact geometry such as the perepoxide-like exciplexes proposed.

These exciplexes could lead to the formation of an intermediate hydroperoxide by preferential abstraction of labile hydrogen geminal to the ester functionality, as it has been shown for the reaction of singlet oxygen with α,β-unsaturated esters [36]. This last intermediate would be responsible for the formation of the main photooxidation product, i.e. the pyridine derivative (Fig. 9, scheme).

The lower nifedipine k_R values (Table 2) can be explained if the labile hydrogen of the 4-position interacts with the nitro group in the *ortho*-position of the 4-aryl substituent, it would not be able to stabilize the negatively charged oxygen of the perepoxide, hindering the formation of the hydroperoxide and permitting the prevalence of the physical deactivation of the singlet oxygen by nifedipine.

4. Conclusions

The results show that nifedipine does not produce $O_2(^1\Delta_g)$ under our experimental conditions. In contrast, this drug behaves as a good scavenger of excited oxygen. The interaction of nifedipine with singlet oxygen is mainly via physical deactivation, while the reactive pathway yielding to nitropyridine product is less privileged ($k_T \gg k_R$).

Nitrendipine generates $O_2(^1\Delta_g)$, but it is a less efficient scavenger of this species than nifedipine. The deactivation of singlet oxygen by nitrendipine is mainly through the reactive channel ($k_T \approx k_R$).

On the other hand, the dependence of rate constants on solvent properties permits us the proposal of the perepoxide-like encounter complex formation with a partial separation of charges. This complex leads to a hydroperoxide and then yields the nitropyridine derivative as the main photooxidation product.

Finally, the present results indicate that nifedipine would have a greater protector effect in biological systems than nitrendipine. Also, it may be concluded that photoallergic and phototoxic effects observed for these drugs could have a different onset.

Acknowledgements

This work was financially supported by FONDECYT, grant no. 3030048. Thanks are also given to the Laboratory of Kinetics and Photochemistry of the Faculty of Chemistry and Pharmaceutical Science of University of Chile, for the use of the facilities. Also, the authors express their gratitude to Professor Fresia Pérez for the English revision.

References

[1] F. Hofmann, V. Flockerzi, W. Nastainczyk, P. Ruth, T. Schneider, Curr. Top. Cell. Regul. 31 (1990) 223–239.
[2] W.A. Catterall, J. Striessnig, Trends Pharmacol. Sci. 13 (1992) 256–262.
[3] R. Berkels, R. Roesen, S. Dhein, U. Fricke, W. Klaus, Cardiovasc. Drug. Res. 17 (1999) 179–186.
[4] X. Zhang, T.H. Hintze, Circulation 97 (1998) 576–580.
[5] L. Cominacini, A.F. Pasini, U. Garbin, A.M. Pastorino, A. Davoli, C. Nava, M. Campagnola, P. Rossato, V. Lo Cascio, Biochem. Biophys. Res. Commun. 302 (2003) 679–684.
[6] I.T. Mak, J.Y. Zhang, W.B. Weglicki, Pharmacol. Res. 45 (2002) 27–33.
[7] L.J. Núñez-Vergara, C. López-Alarcón, P. Navarrete-Encina, A.M. Atria, C. Camargo, J.A. Squella, Free Radic. Res. 37 (2003) 109–120.
[8] C. López-Alarcón, P. Navarrete, C. Camargo, J.A. Squella, L.J. Núñez-Vergara, Chem. Res. Toxicol. 16 (2003) 208–215.
[9] K. Briviba, L.O. Klotz, H. Sies, Biol. Chem. 378 (1997) 1259–1265.
[10] J. Piette, J. Photochem. Photobiol. B: Biol. 11 (1991) 241–260.
[11] H. Sies, C.F.M. Menck, Mutat. Res. 299 (1993) 183–191.
[12] J.R. Wagner, P.A. Motchnik, R. Stocker, H. Sies, B.N. Ames, J. Biol. Chem. 268 (1993) 18502–18506.
[13] B. Epe, M. Pflaum, S. Boiteux, Mutat. Res. 299 (1993) 135–145.
[14] R.A. Floyd, M.S. West, K.L. Eneff, J.E. Schneider, Arch. Biochem. Biophys. 273 (1989) 106–111.
[15] T.P. Devasagayam, S. Steenken, M.S. Obendorf, W.A. Schulz, H. Sies, Biochemistry 30 (1991) 6283–6289.
[16] S. Basu-Modak, R.M. Tyrell, Cancer Res. 53 (1993) 4505–4510.
[17] S. Grether-Beck, S. Olaizola, H. Schimitt, M. Grewe, A. Jahnke, J.P. Johnson, K. Briviba, H. Sies, J. Krutmann, Proc. Natl. Acad. Sci. U.S.A. 93 (1996) 14586–14591.
[18] M. Wlaschek, J. Wenk, P. Brenneisen, K. Briviba, A. Schwarz, H. Sies, K. Scharffetter-Kochanek, FEBS Lett. 413 (1997) 239–242.
[19] Z. Grunwald, Drug Intell. Clin. Pharm. 16 (1982) 492–495.
[20] J. Alcalay, M. David, M. Sandbank, Dermatologica 175 (1987) 191–193.
[21] N.K. Gibbs, N.J. Traynor, B.E. Johnson, J. Ferguson, J. Photochem. Photobiol. B. Biol. 13 (1992) 275–288.
[22] R. Schmidt, C. Tanielian, R. Dunsbach, C. Wolff, J. Photochem. Photobiol. A 79 (1994) 11–17.
[23] J.C. Scaiano, R.W. Redmond, B. Mehta, J.T. Arnanson, Photochem. Photobiol. 52 (1990) 655–659.
[24] I. Mak, P. Boheme, W. Wegliki, Circ. Res. 70 (1992) 1099–1103.
[25] A. Buttafava, A. Faucitano, E. Fasani, A. Albini, A. Ricci, Res. Chem. Intermed. 28 (2002) 231–237.
[26] F. Wilkinson, J. Phys. Chem. Ref. Data. 24 (1995) 663–1021.
[27] C.S. Foote, T.Y. Ching, G.G. Geller, Photochem. Photobiol. 20 (1974) 511–514.
[28] C.S. Foote, Y.C. Chang, R.W. Denny, J. Am. Chem. Soc. 92 (1970) 5216–5218.
[29] L.J. Núñez-Vergara, J.C. Sturm, A. Alvarez-Lueje, C. Olea-Azar, C. Sunkel, J.A. Squella, J. Electrochem. Soc. 146 (1999) 1478–1485.

[30] E. Lemp, A.L. Zanocco, E.A. Lissi, Curr. Org. Chem. 7 (2003) 799–819.
[31] C. Reichardt, Solvents and Solvent Effects in Organic Chemistry, second ed., VCH, Weinheim, 1990.
[32] M.J. Kamlet, J.L. Abboud, M.H. Abraham, R.W. Taft, J. Org. Chem. 48 (1983) 2877–2887.
[33] M. Stratakis, M. Orfanopoulos, Tetrahedron 56 (2000) 1595–1615.
[34] E. Clennan, Tetrahedron 56 (2000) 9151–9179.
[35] Y. Yoshioka, S. Yamada, T. Kawakami, M. Nishino, K. Yamaguchi, I. Saito, Bull. Chem. Soc. Jpn. 69 (1996) 2683–2699.
[36] M. Orfanopoulos, C.S. Foote, Tetrahedron Lett. 26 (1985) 5991–5994.